通过圆偏振光提高飞秒激光诱导击穿光谱的发射强度

于丹[1]，孙艳[1]，冯志书[2]，代玉银[3*]，王秋云[4]，陈安民[4**]，金明星[4***]

[1]空军航空大学航空基础学院，吉林 长春 130022；

[2]空军航空大学作战勤务学院，吉林 长春 130022；

[3]吉林大学第一医院核医学科，吉林 长春 130021；

[4]吉林大学原子与分子物理研究所，吉林 长春 130012

摘要　激光诱导击穿光谱(LIBS)是一种快速、实时的元素成分分析技术。为了提高 LIBS 的灵敏度，人们已经提出多种方法来提高 LIBS 的光谱强度。本文采用飞秒脉冲激光烧蚀黄铜产生 LIBS，对比了圆偏振和线偏振下 LIBS 光谱的强度，结果发现圆偏振下的光谱强度比线偏振下的强，光谱强度大约提高了 15%。采用飞秒激光照射金属时，金属内部的自由电子吸收光子的能量。在线偏振飞秒激光场中，电子在脉冲的每个光学周期中经历交替的加速和减速；而圆偏振飞秒激光可以连续加速电子，因此电子可以获得更高的能量，这使得圆偏振飞秒激光产生的光谱强度不同于线偏振飞秒激光产生的光谱强度，圆偏振激光有助于改善飞秒 LIBS 信号的强度。

关键词　光谱学；激光诱导击穿光谱；飞秒激光；圆偏振；光谱增强

中图分类号　O657.3　　　**文献标志码**　A　　　　　　　　　　**doi**：10.3788/CJL202148.0111001

1　引　　言

激光诱导击穿光谱(LIBS)是一种新颖的原子光谱技术，在材料的元素分析中得到了广泛应用[1-5]。LIBS 采用高功率、短脉冲激光烧蚀样品表面，产生激光诱导的等离子体[6]，等离子体中的原子和离子能辐射出与样品元素组成相关的特征谱线。LIBS 可用于分析任何物质，无论其物理状态是固态、液态还是气态。目前，研究人员正在积极努力地提高 LIBS 的灵敏度，并已提出了许多增强 LIBS 光谱强度的方法，例如：空间约束 LIBS[7]、火花放电辅助 LIBS[8]、纳米粒子增强 LIBS[9]、表面增强 LIBS[10]、偏振分辨 LIBS[11]以及双脉冲 LIBS[12]等。LIBS 有许多优点，如非常低的背景辐射，更快的连续背景衰减，允许大量脉冲信号累加[13]。

随着啁啾脉冲放大飞秒激光技术的发展[14]，飞秒激光系统输出的能量越来越高，飞秒脉冲激光也被引入到 LIBS 的研究中。与纳秒激光相比，飞秒激光的脉冲具有更短的持续时间，能够实现更好的烧蚀深度控制和更高质量的烧蚀坑[15]。此外，飞秒激光可以提高 LIBS 元素分析的性能，例如：可以获得更稳定的光谱信号强度，减弱对待测样品的热损伤，实现更精准的三维元素分析[16]。飞秒激光脉冲的持续时间短于电子与晶格之间的弛豫时间[17]，从而减弱了激光脉冲与等离子体羽之间的相互作用，导致光谱强度相对较弱[18]。因此，提高飞秒 LIBS 的强度是非常必要的。

通常情况下，飞秒激光系统输出的是线偏振的飞秒脉冲激光。在线偏振飞秒激光场中，电子在激光脉冲的每一个光周期内都经历着交替的加减速过程。而圆偏振飞秒激光可以连续加速自由电子，电子将获得更高的能量。由 Kaganov 等[19]在 1957 年和 Anisimov 等[20]在 1974 年提出的双温模型可知，在飞秒激光烧蚀金属过程中，光的吸收主要是由金属内部的类自由电子引起的。因此，圆偏振飞秒激光作用于金属后的自由电子能量将不同于线偏振飞

秒激光作用后的自由电子能量,从而使得圆偏振飞秒激光诱导产生的等离子体的光信号可能不同于线偏振飞秒激光诱导产生的等离子体的光信号。

本文将飞秒激光聚焦到黄铜样品表面进行烧蚀产生等离子体,然后对等离子体光谱进行分析。为了对比线偏振和圆偏振飞秒激光对光谱的影响,利用四分之一波片将飞秒激光的偏振由线偏振调整为圆偏振,测量线偏振和圆偏振飞秒激光诱导黄铜等离子体的时间分辨光谱。结果表明,圆偏振飞秒激光产生的光谱强度高于线偏振下的光谱强度。此外,本文还利用获得的谱线计算了描述等离子体过程的两个重要参数:等离子体的电子温度和电子密度,并对计算结果进行了比较。

2　实验装置

飞秒 LIBS 实验装置示意图如图 1 所示。飞秒激光系统采用的是超快钛蓝宝石放大器,激光系统输出波长为 800 nm 的线偏振脉冲激光,脉冲宽度为 50 fs。通过向飞秒激光系统的同步延时发生器(SDG)的串口(RS232)发送命令(man:trig),可以实现单次模式脉冲激光的输出。利用一个四分之一波片将输出的线偏振激光转变成圆偏振激光,然后通过一个反射镜和一个平凸透镜将线偏振激光或圆偏振激光聚焦到样品(黄铜)表面上,样品置于 PT3-M-Z8 型三维电动平移台上。用一个焦距为 75 mm、直径为 50 mm 的透镜(BK7)收集激光诱导等离子体的光发射,并将收集到的光聚焦到光纤中。光纤将光传输到 SP-500i 型光谱仪上,该光谱仪使用 1200 line/mm 的光栅。光谱色散的光通过一个 ICCD(增强电荷耦合器件)相机进行探测,用 SDG 输出的电信号触发 ICCD 来同步激光与光谱信号之间的延迟,ICCD 将光信号转换成电信号并传输到
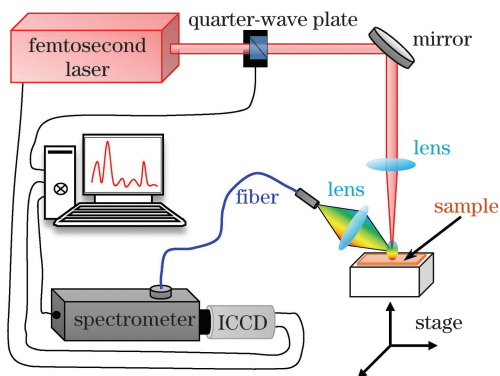
计算机中。每个光谱是 50 个光谱数据的平均值,整个实验在空气中进行。

3　结果与讨论

首先,本文对比了圆偏振和线偏振下飞秒激光诱导黄铜等离子体的时间积分光谱,如图 2 所示,测量的谱线为 468.01 nm、472.21 nm 和 481.08 nm 处的 Zn(Ⅰ)谱线以及 510.55 nm、515.32 nm 和 521.82 nm 处的 Cu(Ⅰ)谱线。从图 2 中可以看出,圆偏振飞秒激光下 Zn(Ⅰ)和 Cu(Ⅰ)的光谱强度明显高于线偏振飞秒下 Zn(Ⅰ)和 Cu(Ⅰ)的光谱强度,约高 15%。飞秒激光场中线偏振和圆偏振的一个重要区别是强激光场作用后自由电子的动能不同:在线偏振激光脉冲中,自由电子在脉冲的每一个光周期内都经历了交替加减速,因而动能较低;相反,在圆偏振激光脉冲中,电子总是被加速,因此获得了更
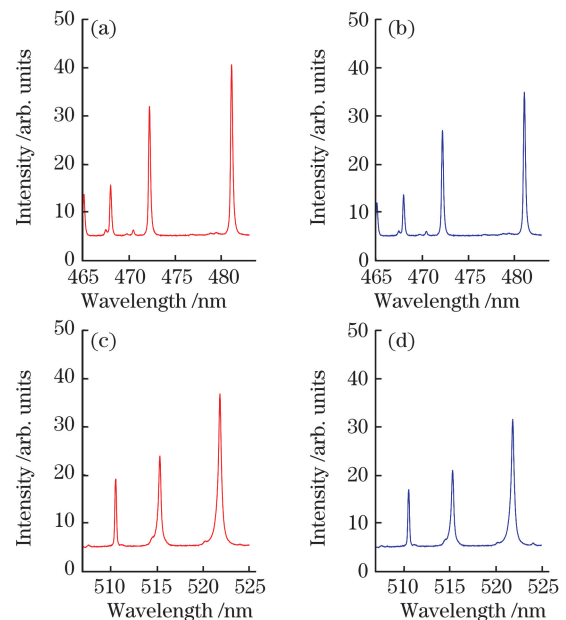

图 2　圆偏振和线偏振下 Zn(Ⅰ)和 Cu(Ⅰ)的时间积分光谱(激光能量为 1.5 mJ)。(a)圆偏振下 Zn(Ⅰ)的时间积分光谱;(b)线偏振下 Zn(Ⅰ)的时间积分光谱;(c)圆偏振下 Cu(Ⅰ)的时间积分光谱;(d)线偏振下 Cu(Ⅰ)的时间积分光谱

Fig. 2　Time-integrated spectra of Zn(Ⅰ)and Cu(Ⅰ)lines with circular and linear polarizations (laser energy is 1.5 mJ). (a) Time-integrated spectrum of Zn(Ⅰ)line with circular polarization; (b) time-integrated spectrum of Zn(Ⅰ)line with linear polarization; (c) time-integrated spectrum of Cu(Ⅰ)line with circular polarization; (d) time-integrated spectrum of Cu(Ⅰ)line with linear polarization

图 1　飞秒 LIBS 实验装置示意图

Fig. 1　Experimental setup of femtosecond LIBS

高的动能[21-22]。在飞秒激光烧蚀过程中,金属的吸收机理是逆轫致辐射吸收过程[23]。飞秒激光照射金属是一个非平衡态的加热过程,在飞秒激光照射金属过程中,金属内的自由电子吸收激光能量,电子的温度迅速升高(金属内电子的热容极低),而晶格的温度几乎保持不变;随着时间延长,电子通过其与晶格之间的耦合将能量转移给晶格,随着晶格温度缓慢升高,金属开始熔化、蒸发直至产生等离子体[24-25]。另外,圆偏振光作用后的电子动能高于线偏振光作用后的电子动能[21,26],而且,圆偏振飞秒激光照射铜靶后,靶内自由电子的能量高于线偏振飞秒激光下的自由电子能量。因此,圆偏振激光将产生更高温度和密度的等离子体,从而产生更强的光谱。

LIBS 是一个动态衰减的过程,在激光产生等离子体之后,LIBS 的光谱辐射强度将会发生变化[27-28]。本文将 ICCD 的门宽设置为 25 ns,测量了飞秒 LIBS 的时间分辨光谱。图 3 给出了圆偏振和线偏振飞秒激光烧蚀黄铜的时间分辨光谱,从中可以看到 0.2 μs 到 1.5 μs 延迟时间范围内 Cu(I) 510.55 nm、Cu(I) 515.32 nm 和 Cu(I) 521.82 nm 的动态衰减过程。在脉冲激光结束后,等离子体开始冷却,等离子体温度和光谱强度开始逐渐降低。圆偏振条件下 Cu(I) 谱线的强度高于线偏振条件下 Cu(I) 谱线的强度,使用圆偏振光可以增加飞秒激光照射金属时的电子动能,
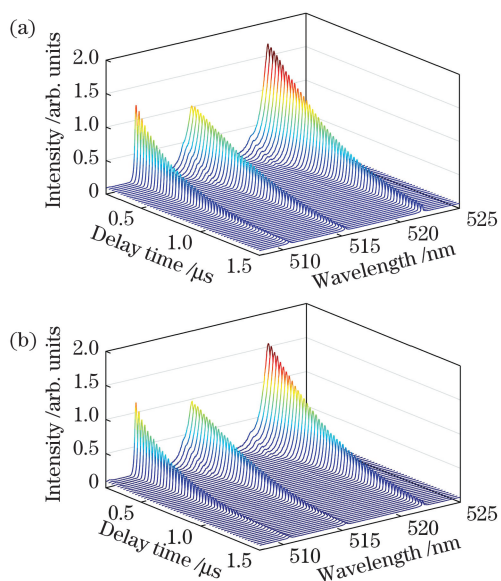

图 3　圆偏振和线偏振下 Cu(I)的时间分辨光谱(激光能量为 1.5 mJ)。(a)圆偏振;(b)线偏振

Fig. 3　Time-resolved spectra of Cu(I) lines with circular and linear polarizations (laser energy is 1.5 mJ). (a) Circular polarization; (b) linear polarization

相比于线偏振激光,电子将具有更高的能量,这等价于增加了入射激光的能量。

为了更清晰地比较偏振对时间分辨光谱的影响,本文选择 Cu(I) 510.55 nm 和 Zn(I) 472.21 nm 讨论不同偏振下的时间分辨光谱。图 4 显示了圆偏振和线偏振飞秒脉冲激光作用下 Cu(I) 510.55 nm 和 Zn(I) 472.21 nm 的峰值强度随着延迟时间的变化,可以看出:圆偏振光下 Cu(I) 510.55 nm 和 Zn(I) 472.21 nm 的峰值强度明显高于线偏振光下的峰值强度,同时圆偏振激光诱导等离子体中原子谱线持续的时间也更长。这表明,圆偏振飞秒脉冲激光能产生更强的等离子体,在等离子体衰减过程中辐射出更强的时间分辨光谱。可见,光的偏振在飞秒 LIBS 中具有重要作用。
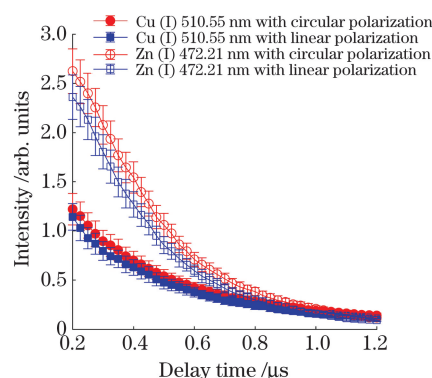

图 4　圆偏振和线偏振下 Cu(I) 510.55 nm 和 Zn(I) 472.21 nm 的峰值强度随着延迟时间的变化(激光能量为 1.5 mJ)

Fig. 4　Evolution of peak intensities of Cu(I) 510.55 nm and Zn(I) 472.21 nm lines with delay time under circular and linear polarizations (laser energy is 1.5 mJ)

飞秒激光脉冲的偏振影响等离子体光谱的机理一直是人们研究的热点。先前的研究发现,不同偏振光作用后的等离子体之间存在一些不同。例如,Lemos 等[29]通过实验证明了圆偏振飞秒激光产生的等离子体羽的膨胀速度比线偏振光的快。众所周知,飞秒激光脉冲可以通过电离激发等离子体,这就是所谓的阈上电离。电离电子的速度是由电离时激光电场的相位决定的,当电子被电离成自由电子时,电子获得的能量与电场的相位有关。Corkum 等[30]指出,通过改变电离激光脉冲的偏振和波长可以控制等离子体的电子温度。他们还计算了圆偏振和线偏振下激光诱导等离子体的电子能谱,结果发现,圆偏振激光作用后的能谱更宽,而且圆偏振激光会产

生更高的等离子体温度,从而加速了等离子体的膨胀。因此,圆偏振光能使电子获得更高的能量[31-32],在圆偏振条件下等离子体内的电子与原子或离子之间的碰撞更为频繁,从而导致等离子体的密度更大。为了验证上述讨论,本文测量了不同偏振激光脉冲在不同激光能量下激发的铜等离子体的光谱强度分布,结果如图 3 所示。可以看出,在圆偏振情况下,铜等离子体的密度较高。此外,本文还计算了圆偏振和线偏振下飞秒脉冲激光产生的等离子体的电子温度和电子密度。

假设激光诱导等离子体处于局部热力学平衡和光学薄的状态,采用 Boltzmann 图法可以很容易计算出等离子体的电子温度,计算公式为

$$\ln\left(\frac{I\lambda}{A_{ki}g_k}\right) = -\frac{E_k}{k_B T_e} + C, \tag{1}$$

式中:I 为强度;λ 为波长;k 和 i 分别表示上下能级;A_{ki} 为跃迁概率;g_k 为上能级简并;E_k 为上能级能量;k_B 为 Boltzmann 常数;T_e 为等离子体的电子温度;C 为常数。光谱参数 g_k、A_{ki} 和 E_k 都来自 NIST 数据库,见表 1[33-34]。

表 1 Cu (I)光谱线对应的相关参数值
Table 1 Spectral parameters of Cu (I)

Line	Wavelength /nm	Transition	$A_{ki}g_k$	E_k/eV
Cu (I)	510.55	$3d^{10}4p(^2P_{3/2}) - 3d^94s^2(^2D_{5/2})$	8.0×10^6	3.82
Cu (I)	515.32	$3d^{10}4d(^2D_{3/2}) - 3d^{10}4p(^2P_{1/2})$	2.4×10^8	6.19
Cu (I)	521.82	$3d^{10}4d(^2D_{5/2}) - 3d^{10}4p(^2P_{3/2})$	4.5×10^8	6.19

选择 Cu(I) 510.55 nm、Cu(I) 515.32 nm 和 Cu(I) 521.82 nm 谱线建立用于等离子体电子温度计算的 Boltzmann 图,因为这三条谱线具有较宽的能级范围,可以大大提高计算等离子体电子温度的准确性[35]。典型的线性 Boltzmann 图如图 5 所示。结合(1)式和表 1 计算 $\ln[\lambda I/(A_{ki}g_k)]$ 和 E_k 的值,然后将这些数据点进行线性拟合,拟合结果如图 5 所示。

Stark 展宽成为谱线加宽的主要展宽过程。谱线宽度和等离子体中电子的数密度之间的关系为

$$\Delta\lambda_{1/2} \approx 2 \times 10^{-16}\omega N_e, \tag{2}$$

式中:$\Delta\lambda_{1/2}$ 为谱线宽度;ω 为电子的碰撞参数;N_e 为电子的数密度。谱线展宽包括 Doppler 展宽($\Delta\lambda^D_{FWHM}$)、仪器展宽($\Delta\lambda_{instrument}$)和自然展宽($\Delta\lambda^N_{FWHM}$),它们之间的关系是 $\Delta\lambda_{1/2} = \Delta\lambda_{observed} - \Delta\lambda_{instrument} - \Delta\lambda^D_{FWHM} - \Delta\lambda^N_{FWHM}$,其中 $\Delta\lambda_{observed}$ 是通过拟合实验数据得到的线宽。在实验中,通过测量低压汞灯发射谱线确定的仪器展宽约为 0.04 nm,Doppler 展宽和自然展宽都可以忽略,因此有 $\Delta\lambda_{1/2} = \Delta\lambda_{observed} - \Delta\lambda_{instrument}$。图 6 展示了圆偏振下延迟时间分别为 0.4 μs 和 0.5 μs 时 Cu (I) 510.55 nm 谱线的 Stark 展宽轮廓。
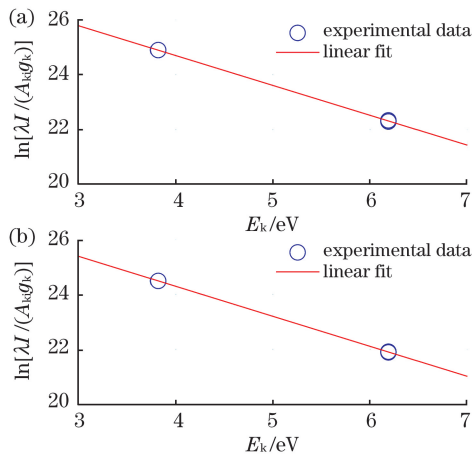
图 5 典型的 Boltzmann 图。(a)圆偏振,延迟时间为 0.4 μs;(b)圆偏振,延迟时间为 0.5 μs

Fig. 5 Typical Boltzmann plots. (a) Circular polarization, delay time of 0.4 μs; (b) circular polarization, delay time of 0.5 μs
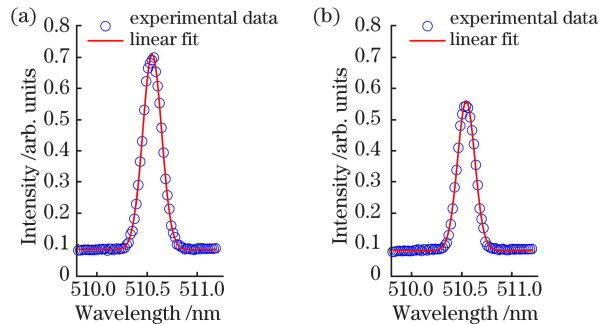
在 LIBS 中,可以忽略除 Stark 展宽之外的其他展宽机制,例如 Doppler 展宽和自然展宽。因此,

图 6 Cu(I) 510.55 nm 谱线的 Stark 展宽轮廓。(a)圆偏振,延迟时间为 0.4 μs;(b)圆偏振,延迟时间为 0.5 μs

Fig. 6 Stark broadening frofile of Cu (I) 510.55 nm spectral line. (a) Circular polarization, delay time of 0.4 μs; (b) circular polarization, delay time of 0.5 μs

图 7 为圆偏振和线偏振飞秒激光诱导的黄铜等离子体的电子温度和电子密度随延迟时间的变化。等离子体电子温度和电子密度的变化与光谱强度的变化(图 4)相似,圆偏振激光脉冲作用后的电子与原子或离子的碰撞会导致更高的电子密度和电子温度。圆偏振下等离子体的电子温度和电子密度高于线偏振下等离子体的电子温度和电子密度。如上所述,圆偏振激光可以不断地加速电子使其获得更多的能量,更多的能量被转移到晶格上,产生更强的等离子体。相比线偏振激光,圆偏振光下等离子体的电子温度更高,相应的电子密度也更高。
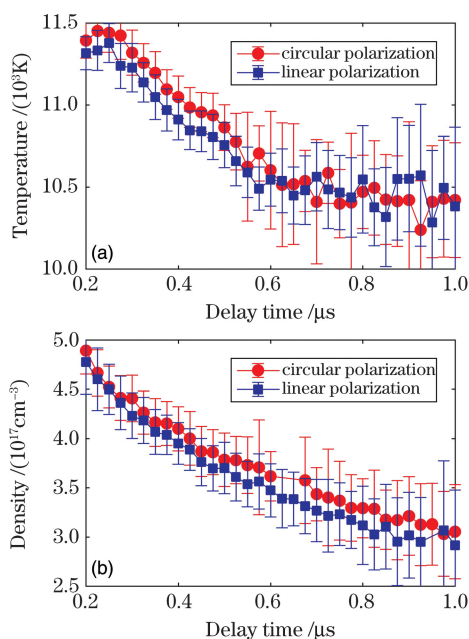

图 7 圆偏振和线偏振下电子温度和电子密度随着延迟
时间的变化(激光能量为 1.5 mJ)。(a)电子温度;
(b)电子密度

Fig. 7 Evolution of electron temperature and density
with delay time under circular and linear
polarizations(laser energy is 1.5 mJ). (a) Electron
temperature; (b) electron density

4 结 论

本文通过聚焦飞秒脉冲激光到黄铜样品表面产生等离子体,测量了线偏振和圆偏振下等离子体辐射的 Zn (I)和 Cu (I)原子谱线。结果表明,圆偏振光下的谱线强度高于线偏振光下的谱线强度,谱线强度大约提高了 15%。本文还测量了线偏振和圆偏振飞秒激光诱导黄铜等离子体的时间分辨光谱,在激光能量相同的情况下,圆偏振激光诱导等离子体中原子谱线的持续时间较长;同时,本文利用测量

的 Cu (I)线获得了时间分辨的等离子体电子温度和电子密度,结果表明,与线偏振相比,圆偏振下等离子体的电子温度和电子密度也较高。这是由于圆偏振激光能不断地加速电子,圆偏振飞秒激光脉冲作用后的电子动能高于线偏振光作用后的电子动能,动能较高的电子在等离子体中碰撞,产生更高温度和密度的等离子体,从而产生更高的光谱强度。因此,可以采用将线偏振激光调整成圆偏振激光的方法提高飞秒 LIBS 光谱信号的强度。希望本工作能为飞秒 LIBS 的研究提供有益的参考。

参 考 文 献

[1] Wang Z, Dong F Z, Zhou W D. A rising force for the world-wide development of laser-induced breakdown spectroscopy [J]. Plasma Science and Technology, 2015, 17(8): 617-620.

[2] Jia J W, Fu H B, Wang H D, et al. Improvement of beam shape modification on stability of laser induced breakdown spectroscopy [J]. Chinese Journal of Lasers, 2019, 46(3): 0311004.
贾军伟, 付洪波, 王华东, 等. 光束整形对激光诱导击穿光谱稳定性的改善[J]. 中国激光, 2019, 46(3): 0311004.

[3] Liu S M, Xiu J S, Liu Y Y. Rapid quantitative analysis of element content ratios in Cu(in, Ga)Se₂ thin films using laser-induced breakdown spectroscopy[J]. Chinese Journal of Lasers, 2019, 46(9): 0911001.
刘世明, 修俊山, 刘云燕. 基于激光诱导击穿光谱技术的铜铟镓硒薄膜中元素含量比的快速定量分析方法[J]. 中国激光, 2019,46(9): 0911001.

[4] Yang X, Zhang D, Chen A M, et al. Influence of distance between focusing lens and sample surface on atomic line and ionic line intensities of laser-induced silicon plasmas[J]. Chinese Journal of Lasers, 2019, 46(11): 1111001.
杨雪, 张丹, 陈安民, 等. 聚焦透镜到样品表面的距离对激光诱导硅等离子体原子谱线强度和离子谱线强度的影响[J]. 中国激光, 2019, 46(11): 1111001.

[5] Zheng P C, Li Q Y, Wang J M, et al. Detection of copper and manganese in water by laser-induced breakdown spectroscopy based on chelate resin[J]. Chinese Journal of Lasers, 2019, 46(8): 0811001.
郑培超, 李倩雨, 王金梅, 等. 螯合树脂富集辅助激光诱导击穿光谱检测水体中的 Cu 元素和 Mn 元素[J]. 中国激光, 2019, 46(8): 0811001.

[6] Qi H X, Zhao L, Jin C L, et al. Influence of sample temperature on spectral intensity of nanosecond laser-induced aluminum plasma [J]. Chinese Journal of Lasers, 2019, 46(2): 0211002.

齐洪霞，赵亮，金川琳，等. 样品温度对纳秒激光诱导铝等离子体光谱强度的影响[J]. 中国激光，2019，46(2)：0211002.

[7] Wang Y, Yuan H, Fu Y T, et al. Experimental and computational investigation of confined laser-induced breakdown spectroscopy [J]. Spectrochimica Acta Part B: Atomic Spectroscopy, 2016, 126: 44-52.

[8] Wang Q Y, Chen A M, Wang Y, et al. Spectral intensity clamping in linearly and circularly polarized femtosecond filament-induced Cu plasmas [J]. Journal of Analytical Atomic Spectrometry, 2018, 33 (7): 1154-1157.

[9] Dell′Aglio M, Alrifai R, De Giacomo A. Nanoparticle enhanced laser induced breakdown spectroscopy (NELIBS), a first review [J]. Spectrochimica Acta Part B: Atomic Spectroscopy, 2018, 148: 105-112.

[10] Aguirre M A, Legnaioli S, Almodóvar F, et al. Elemental analysis by surface-enhanced laser-induced breakdown spectroscopy combined with liquid-liquid microextraction [J]. Spectrochimica Acta Part B: Atomic Spectroscopy, 2013, 79/80: 88-93.

[11] Penczak J S, Liu Y M, Gordon R J. Polarization and fluence dependence of the polarized emission in nanosecond laser-induced breakdown spectroscopy [J]. Spectrochimica Acta Part B: Atomic Spectroscopy, 2011, 66(2): 186-188.

[12] Wang Y, Chen A M, Zhang D, et al. Enhanced optical emission in laser-induced breakdown spectroscopy by combining femtosecond and nanosecond laser pulses [J]. Physics of Plasmas, 2020, 27(2): 023507.

[13] Wang Y, Chen A M, Li S C, et al. Enhancement of laser-induced Fe plasma spectroscopy with dual-wavelength femtosecond double-pulse[J]. Journal of Analytical Atomic Spectrometry, 2016, 31(2): 497-505.

[14] Strickland D, Mourou G. Compression of amplified chirped optical pulses[J]. Optics Communications, 1985, 56(3): 219-221.

[15] Wang Q, Chen A, Li S, et al. Influence of ambient pressure on the ablation hole in femtosecond laser drilling Cu[J]. Applied Optics, 2015, 54(27): 8235-8240.

[16] Hou H M, Cheng L, Richardson T, et al. Three-dimensional elemental imaging of Li-ion solid-state electrolytes using fs-laser induced breakdown spectroscopy (LIBS) [J]. Journal of Analytical Atomic Spectrometry, 2015, 30(11): 2295-2302.

[17] Wang T F, Guo J, Shao J F, et al. Ultrafast thermionic emission from metal irradiated using a femtosecond laser and an electric field in combination [J]. Physics of Plasmas, 2015, 22(3): 033106.

[18] Freeman J R, Harilal S S, Diwakar P K, et al. Comparison of optical emission from nanosecond and femtosecond laser produced plasma in atmosphere and vacuum conditions[J]. Spectrochimica Acta Part B: Atomic Spectroscopy, 2013, 87:43-50.

[19] Kaganov M I, Lifshitz M I, Tanatarov M V. Relexation between electrons and cristialline lattices [J]. Soviet Physics JETP, 1957, 4: 173-178.

[20] Anisimov S I, kapeliovish B L. Electron emission from metal surfaces exposed to ultra-short laser pulses[J]. Soviet Physics JETP, 1974, 39: 375-378.

[21] Li S Y, Li S C, Sui L Z, et al. Contribution of nitrogen atoms and ions to the luminescence emission during femotosecond filamentation in air[J]. Physical Review A, 2016, 94(5): 059901.

[22] Mitryukovskiy S, Liu Y, Ding P J, et al. Plasma luminescence from femtosecond filaments in air: evidence for impact excitation with circularly polarized light pulses[J]. Physical Review Letters, 2015, 114(6): 063003.

[23] Qi H X, Li S Y, Qi Y, et al. Effect of sample position on collinear femtosecond double-pulse laser-induced breakdown spectroscopy of silicon in air[J]. Journal of Analytical Atomic Spectrometry, 2014, 29 (6): 1105-1111.

[24] Guo J, Wang T F, Shao J F, et al. Emission enhancement ratio of the metal irradiated by femtosecond double-pulse laser [J]. Optics Communications, 2012, 285(7): 1895-1899.

[25] Li S C, Li S Y, Jiang Y F, et al. Electron emission from a double-layer metal under femtosecond laser irradiation[J]. Nuclear Instruments and Methods in Physics Research Section B: Beam Interactions With Materials and Atoms, 2015, 342: 300-304.

[26] Shi Y, Chen A M, Jiang Y F, et al. Influence of laser polarization on plasma fluorescence emission during the femtosecond filamentation in air [J]. Optics Communications, 2016, 367: 174-180.

[27] Ahmed R, Ahmed N, Iqbal J, et al. An inexpensive technique for the time resolved laser induced plasma spectroscopy[J]. Physics of Plasmas, 2016, 23(8): 083101.

[28] Wang Q Y, Chen A M, Xu W P, et al. Signal improvement using circular polarization for focused femtosecond laser-induced breakdown spectroscopy [J]. Journal of Analytical Atomic Spectrometry, 2019, 34(6): 1242-1246.

[29] Lemos N, Grismayer T, Cardoso L, et al. Effects of laser polarization in the expansion of plasma waveguides[J]. Physics of Plasmas, 2013, 20(10):

103109.

[30] Corkum P B, Burnett N H, Brunel F. Above-threshold ionization in the long-wavelength limit[J]. Physical Review Letters, 1989, 62(11): 1259-1262.

[31] Smeenk C T, Arissian L, Zhou B, et al. Partitioning of the linear photon momentum in multiphoton ionization[J]. Physical Review Letters, 2011, 106 (19): 193002.

[32] Zhou B, Houard A, Liu Y, et al. Measurement and control of plasma oscillations in femtosecond filaments[J]. Physical Review Letters, 2011, 106 (25): 255002.

[33] Nakimana A, Tao H Y, Gao X, et al. Effects of ambient conditions on femtosecond laser-induced breakdown spectroscopy of Al[J]. Journal of Physics D: Applied Physics, 2013, 46(28): 285204.

[34] Ciucci A, Corsi M, Palleschi V, et al. New procedure for quantitative elemental analysis by laser-induced plasma spectroscopy [J]. Applied Spectroscopy, 1999, 53(8): 960-964.

[35] Zorba V, Mao X L, Russo R E. Femtosecond laser induced breakdown spectroscopy of Cu at the micron/sub-micron scale[J]. Spectrochimica Acta Part B: Atomic Spectroscopy, 2015, 113: 37-42.

Improving Emission Intensity of Femtosecond Laser-Induced Breakdown Spectroscopy by Using Circular Polarization

Yu Dan[1], Sun Yan[1], Feng Zhishu[2], Dai Yuyin[3*], Wang Qiuyun[4], Chen Anmin[4**], Jin Mingxing[4***]

[1] Basic Aviation College, Air Force Aviation University, Changchun, Jilin 130022, China;

[2] Aviation Operations Service College, Air Force Aviation University, Changchun, Jilin 130022, China;

[3] Nuclear Medicine Department, the First Hospital of Jilin University, Changchun, Jilin 130021, China;

[4] Institute of Atomic and Molecular Physics, Jilin University, Changchun, Jilin 130012, China

Abstract

Objective Laser-induced breakdown spectroscopy (LIBS) is a novel atomic-emission spectroscopic technique that has been widely used for the elemental analysis of materials. Investigators in the field of LIBS research are actively working to improve the sensitivity of this technique, and many methods have been proposed to enhance its spectral intensity. With the development of chirped-pulse-amplification technology, femtosecond pulse lasers have been introduced into the study of LIBS. Compared with nanosecond lasers, femtosecond lasers have many advantages for LIBS, but it is important to improve their spectral intensity. In general, the output laser beam of a femtosecond laser system is linearly polarized. In a linearly polarized laser field, electrons undergo alternating acceleration and deceleration in each optical period of the laser pulse. However, femtosecond lasers with circular polarization can accelerate electrons continuously, so they attain higher energies. The energies of electrons after irradiation with a circularly polarized femtosecond laser beam are different from those of electrons after irradiation with a linearly polarized femtosecond laser beam. This makes the optical signal from a plasma induced by a circularly polarized femtosecond laser beam different from that induced by a linearly polarized femtosecond laser beam. It is therefore necessary to compare the plasma emission induced by a femtosecond laser under both linear and circular polarizations.

Methods We focused a femtosecond laser beam onto the surface of a brass sample to produce plasmas, and we analyzed the resulting plasma spectra. To compare the effects of linear and circular polarizations on the spectral-emission intensity, we adjusted the polarization of the femtosecond laser beam from linear polarization to circular polarization by using a quarter-wave plate. The sample was placed on a three-dimensional translation table to avoid over-ablation. We collected the light emission from the laser-induced plasma and focused the collected light into an optical fiber, which transmitted it to a spectrometer. The light dispersed by the spectrometer was detected with an intensified charge-coupled device (ICCD). The ICCD was synchronized using an electrical signal from the synchronization-and-delay generator of the femtosecond laser system. Each spectral datum was an average of 50 laser shots. The whole experiment was carried out in air.

Results and Discussions We first compared the time-integrated spectra from femtosecond-laser-induced brass

plasmas obtained under circular and linear polarizations. The spectral intensities of Zn (I) and Cu (I) obtained with a circularly polarized laser beam were higher than those obtained with a linearly polarized laser beam, and the spectral intensity increased by about 15％. An important difference between linear polarization and circular polarization in the femtosecond laser field is that the kinetic energies of electrons subject to differently polarized laser fields are different. Under linear polarization, electrons undergo alternating acceleration and deceleration in each optical period of the pulse, so they attain low kinetic energy. In contrast, electrons are always accelerated under circular polarization, so they attain high kinetic energy. Second, we measured the time-resolved spectra of femtosecond LIBS. The time-resolved peak intensities of Cu (I) at 510.55 nm and Zn (I) at 472.21 nm under circularly polarized laser are higher than that under linearly polarized laser, and the atomic lines in circularly polarized laser-induced plasmas persist longer duration. We thus find that circularly polarized femtosecond pulsed laser irradiation can produce stronger plasmas, which emitting stronger time-resolved spectra during the process of plasma decay. Laser polarization thus plays an important role in femtosecond LIBS. Finally, we calculated the time-resolved electron temperature and density under irradiation with circular and linear polarizations based on the Boltzmann plot and Stark broadening. The changes in the electron temperature and density are similar to the changes in the spectral intensity. Electrons under circularly polarized laser collide with atoms or ions, leading to higher electron temperature and density than those under linearly polarized laser. The higher-energy electrons transfer more energy to the lattice to produce stronger plasmas.

Conclusions　We produced plasmas on the surfaces of brass samples by using focused femtosecond pulse laser, and we measured the spectral lines of Zn (I) and Cu (I) emitted from the plasmas under linear and circular polarizations. The results show that the spectral intensities under circularly polarized femtosecond laser were higher than those under linearly polarized femtosecond laser, and the spectral intensities increased by about 15％. We also measured the time-resolved spectra of linearly and circularly polarized femtosecond-laser-induced brass plasmas. For the same laser energy, atomic lines in the plasma produced by the circularly polarized laser persisted longer duration than those produced by the linearly polarized laser. Compared with linear polarization, the electron temperature and density obtained with circular polarization were also higher. This is because a circularly polarized laser can accelerate the electrons continuously, so the kinetic energy of electron produced by a circularly polarized femtosecond laser are higher than that produced by a linearly polarized femtosecond laser. Electrons with higher kinetic energy collide in the plasma to produce higher electron temperature and density, which thus emit a higher spectral intensity. Therefore, we can improve the signal intensity of femtosecond LIBS by adjusting a femtosecond laser from linear polarization to circular polarization. We expect this work to be useful for the study of femtosecond LIBS.

Key words　spectroscopy；laser-induced breakdown spectroscopy；femtosecond laser；circular polarization；spectral enhancement

OCIS codes　300.6365；300.2140；070.4790